



How low-velocity non-Darcian flow in low-permeability media controls the leakage characteristics of a leaky aquifer system

Xianmeng Meng¹ · Ge Yan¹ · Lintao Shen¹ · Maosheng Yin² · Dengfeng Liu³

Received: 7 April 2023 / Accepted: 23 December 2023 / Published online: 10 January 2024
© The Author(s), under exclusive licence to International Association of Hydrogeologists 2024

Abstract

The distribution of saline water in the upper aquifer and freshwater in the lower aquifer is a characteristic of groundwater resources in the North China Plain (NCP). The phenomenon of groundwater depression cones in confined aquifers, primarily caused by excessive groundwater extraction, has been extensively documented. In line with Darcy's law, it is noteworthy that the migration of shallow groundwater into confined aquifers can occur due to a substantial difference in hydraulic head between the unconfined and confined aquifer systems. However, based on the monitoring data, the quality of deep groundwater generally remains good. This paper attempts to explain this phenomenon from the perspective of non-Darcian flow in aquitards. A finite difference method is used to solve low-velocity non-Darcian flow to a well in the NCP. The mathematical model considers the threshold pressure gradient to describe non-Darcian flow in the aquitard and assumes Darcian and horizontal flows for both shallow and confined aquifers. The comparison with traditional Darcian flow indicates that the leaky area decreases rapidly when considering the threshold pressure gradient. The leaky area is negatively correlated with the aquitard thickness and the transmissivity of the confined aquifer, and positively correlated with the pumping rate. The non-Darcian vertical flow velocity is significantly lower than that obtained from Darcian theory. The vertical velocity difference between Darcian and non-Darcian flows is significant under the situation of a small aquitard thickness, large pumping rate, low transmissivity and large leakage coefficient when the threshold pressure gradient is large.

Keywords Non-Darcian flow · Aquitard · Groundwater flow · Threshold pressure gradient · Leaky aquifer

Introduction

Water is a crucial resource for the sustainable development of modern society and its economy, with groundwater playing an important part. Groundwater not only compensates for the shortage of regional water supply due to uneven distribution of surface-water resources, but it also maintains ecological balance (Yu et al. 2018). The North China Plain

faces severe water scarcity (Shi et al. 2011). Surface-water resources in this region are limited, accounting for only 1.9% of China's total water resources (Chen 2010), while about two-fifths of China's population resides there. Consequently, groundwater has become the main source of water (Wang et al. 2018), representing 70% of the total water supply (Zheng et al. 2010). The geological and hydrogeological conditions in the region are characterized by multi-layer aquifer systems comprising shallow and confined aquifers and clay layers. Due to various geological factors and processes—such as paleogeography, paleoclimate, Quaternary glacial and interglacial periods, transgression-regression cycles, and evaporation dissolution—the shallow groundwater has been mineralized to become saline water (Cao et al. 2016; Yi et al. 2016; Han et al. 2020). The North China Plain is known for the phenomenon of saline water in the upper aquifer and freshwater in the lower aquifer (Su et al. 2018; Shi et al. 2019). Owing to the poor quality of shallow groundwater and low yield from individual shallow wells, deep groundwater is the primary source of water supply.

✉ Xianmeng Meng
mengxianmeng2000@163.com

¹ School of Environmental Studies, China University of Geosciences, Wuhan 430074, China

² School of Environmental Science and Engineering, Southern University of Science and Technology, Shenzhen 518055, China

³ State Key Laboratory Base of Eco-hydraulic Engineering in Arid Area, School of Water Resources and Hydropower, Xi'an University of Technology, Xi'an 710048, China

The North China region is experiencing a continuous increase in water demand due to the rapid growth of industry and agriculture, resulting in constant overexploitation of groundwater resources (Chen et al. 2003; Shi et al. 2011; Jiang et al. 2018). The long-term decline in groundwater levels has led to the formation of a large regional groundwater depression cone, causing a series of environmental geological problems such as land subsidence, down-movement of the fresh–saline groundwater interface, seawater intrusion, and ground fissures (Liu et al. 2001; Chen et al. 2020; Liu et al. 2020). This situation poses significant challenges to domestic water supply, food security, and the stability of engineering structures (Foster et al. 2004). Furthermore, the hydraulic connection between the upper saline water and deep freshwater is being strengthened by the continuous expansion of the deep groundwater depression cone (Li et al. 2016). The leaky recharge of shallow saline groundwater into the deep fresh aquifer under a large vertical hydraulic gradient increases the risk of salinization, further threatening the security of safe water supply.

Movement of an upper saline water boundary into a confined aquifer under a large head difference is a significant concern in terms of hydrogeology; thus, according to Darcy's law, a large amount of shallow groundwater in the North China Plain is expected to enter the confined aquifer due to the large head difference. While the shallow groundwater is saline, the recharge to the confined aquifer may have great impact on the deep aquifer; however, the quality of deep groundwater in the North China Plain has not deteriorated significantly, and the total dissolved solids content has not increased significantly. Some researchers have studied this phenomenon and offered explanations—for example, Wang (2002) investigated the characteristics of the multilayer aquifer system in the city of Tianjin and concluded that the interaction between micro clay particles of the calcified clay in the aquitard and the aqueous solution prevented the downward migration of saline water. Zuo and Wan (2006) analyzed the hydrodynamic and hydrochemical field characteristics under the exploitation conditions in the plain region of Tianjin and found that delayed leakage in the clay layer significantly reduced the downward-movement velocity of the saline groundwater. Shi et al. (2014) verified the existence of interaction between micro clay particles of calcified clay in the aquitard and the aqueous solution through leakage tests using a closed undisturbed soil infiltration device. Li et al. (2016) selected a typical profile of the domain in Hengshui to analyze the groundwater quality characteristics and evolution of the multilayer aquifer system, and found that the leakage from the shallow aquifer to the confined aquifer was limited even if the head difference was over 40 m.

Aquitards are continuously distributed throughout the North China Plain and act as protective layers for the confined aquifer to prevent contamination and salinization (Li

et al. 2013; Han et al. 2021). The downward migration of saline water is influenced not only by the head difference and the solute concentration of the shallow saline groundwater, but also by the thickness and lithology of the aquitard. Clay, the main component of the aquitard, is a typical low-permeability medium that controls the seepage flow and the characteristics of solute transport in a leaky aquifer system. However, water flow in low-permeability media differs significantly from traditional Darcian flow (Liu et al. 2013), which has been reported by many scholars (Nilson 1981; Liu and Birkholzer 2012; Liu et al. 2012; Cai 2014; Chen 2019). Subsequently, researchers have studied the impact of low-velocity non-Darcian flow on groundwater flow and solute transport—for example, Zhu et al. (2006, 2007) studied the impact of the threshold pressure gradient and moving boundary on solute transport in low-permeability media using a one-dimensional (1D) soil column experiment. Cui et al. (2014) investigated the consolidation process produced by low-velocity non-Darcian flow during saline water downward migration in the North China Plain. Meng et al. (2015) studied the impact of low-velocity non-Darcian flow in the first kind of leaky aquifer system (ignoring the storage capacity of the aquitard) on the determination of hydrogeological parameters. Zhu et al. (2020) derived a new solution to the transient single-well push-pull test with low-permeability non-Darcian leakage effects.

To the authors' knowledge, most existing research on low-velocity non-Darcian flow has mainly focused on simulating one-dimensional seepage in soil columns (Li et al. 2012; Liu et al. 2012, 2013; Hu et al. 2022; Teng et al. 2023). Only rarely has research explored the influence of non-Darcian flow on the whole leaky aquifer system. Even when the low-velocity non-Darcian flow equation is coupled with equations of groundwater flow in aquifers, the assumption is that the shallow groundwater level remains constant during the pumping period, which differs significantly from the actual situation and can impact the reliability of the results.

The objective of this study is to investigate the reasons for the absence of large-scale salinization in confined aquifers from the perspective of the laws governing water movement. To achieve this, the low-velocity non-Darcian flow equation is coupled with the equations of groundwater flow in aquifers with a radial coordinate system, and changes in the shallow groundwater level during pumping periods are considered. According to previous research (Han et al. 2021), most of the groundwater samples taken in the North China Plain have total dissolved solids concentrations of less than 5 g/L, which is about one-seventh of the seawater or saline lakes. The difference between the real flow system and numerical simulation caused by the neglect of density-dependent flow will be less than 0.5%, a difference that is expected to have little impact on the conclusions in this study (Simmons 2005). According to the relationship

between groundwater solute concentration and viscosity proposed in Ophori (1998), the variation caused by solute concentration is quite limited when the concentration is less than 1 mol/L. For the total dissolved solids of groundwater in the North China Plain, 5 g/L corresponds to a concentration of 0.0856 mol/L for NaCl; therefore, the variation of viscosity of the groundwater in the North China Plain can be neglected. Additionally, the average depth to the top of the aquitard in the North China Plain is reported to be 60 m (Cao 2013), at which depth the temperature of groundwater remains stable or varies very slowly. For the aforementioned reasons, nondense and nonviscous flow was considered in this study. The differences between the results obtained using Darcian and non-Darcian flows are analyzed, and their influencing factors are identified under the condition of a well fully penetrating a confined aquifer. The numerical model proposed in this study allows one to investigate the impact of low-velocity non-Darcian flow on the overall groundwater system at a larger scale in a more realistic way.

Statement of the problem

Mathematical model

Based on the distribution of aquifers and the characteristics of saline and freshwater in the North China Plain, a leaky aquifer system consisting of three layers—shallow aquifer, aquitard, and confined aquifer—is simplified and schematically shown in Fig. 1. To make the problem more mathematically tractable, this study makes assumptions similar to those used in Hantush and Jacob (1955): each layer is homogenous and laterally infinite; the storage capacity of the aquitard is ignored;

the heads of both the shallow aquifer and confined aquifer are the same before pumping starts; the pumping rate of the well fully penetrating the confined aquifer is constant; flows in the aquifers are horizontal and follow Darcy’s law; and flow in the aquitard is vertical. To describe the low-velocity non-Darcian behavior in the aquitard, a threshold pressure gradient is used, and the flux-gradient relationship is given as (Liu and Birkholzer 2012):

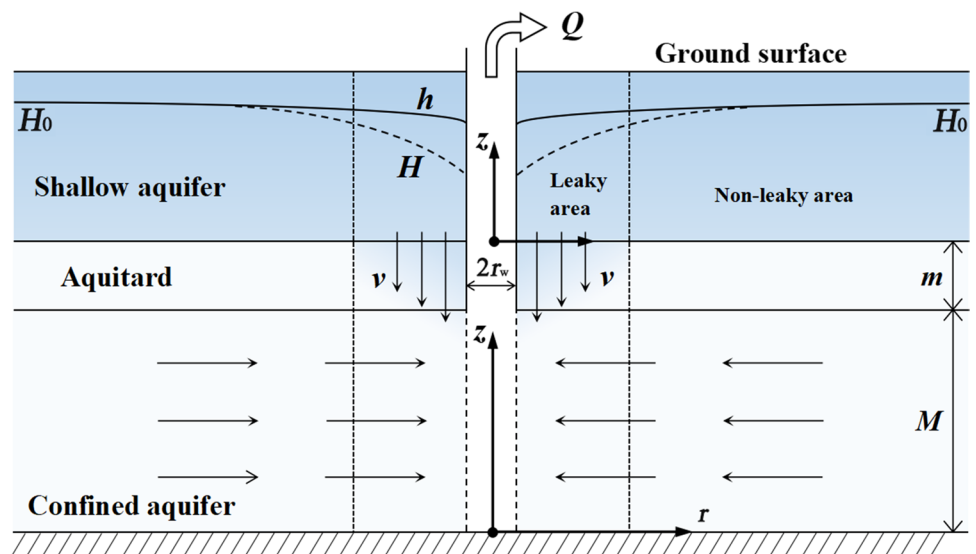
$$v = \begin{cases} 0 & i \leq i_0 \\ K_v(i - i_0) & i > i_0 \end{cases} \tag{1}$$

where v is the vertical flow velocity [LT^{-1}]; K_v is the vertical hydraulic conductivity of the aquitard [LT^{-1}]; i and i_0 are the vertical hydraulic gradient and the threshold pressure gradient, respectively. The low-velocity non-Darcian law described by Eq. (1) was widely used in previous studies, due to its simplicity and ease of use (Luo et al. 2019). When $i_0 = 0$, Eq. (1) is reduced to the traditional Darcy’s law. In this study, groundwater flow described by Darcy’s law was referred to as Darcian flow, while other flows that could not be described by Darcy’s law were termed as non-Darcian flow.

Based on the flux-gradient relationship described in the preceding, the entire region can be divided into two parts: the leaky area and the nonleaky area. A cylindrical coordinate system is established with the origin located at the intersection of the well center axis and the bottom of the confined aquifer. The governing equations for groundwater flow in the confined aquifer under cylindrical coordinates can be expressed as:

$$\frac{\partial^2 H}{\partial r^2} + \frac{1}{r} \frac{\partial H}{\partial r} + \frac{K_v}{T}(i - i_0) = \frac{S}{T} \frac{\partial H}{\partial t} \quad (i > i_0) \tag{2}$$

Fig. 1 Schematic of a single pumping well fully penetrating the confined aquifer shown in vertical profile



$$\frac{\partial^2 H}{\partial r^2} + \frac{1}{r} \frac{\partial H}{\partial r} = \frac{S}{T} \frac{\partial H}{\partial t} \quad (i \leq i_0) \quad (3)$$

$$H(r, 0) = H_0 \quad (4)$$

$$\lim_{r \rightarrow r_w} 2\pi r T \frac{\partial H}{\partial r} = Q \quad (5)$$

$$H(r \rightarrow +\infty, t) = H_0 \quad (6)$$

where H and H_0 are the groundwater head and initial head in the confined aquifer, respectively [L]; r is the radial distance from the pumping well [L]; r_w is the well radius [L]; T is the transmissivity of the confined aquifer [$L^2 T^{-1}$], which can be expressed as $T = K_2 M$, for which K_2 is the hydraulic conductivity of the confined aquifer [$L T^{-1}$] and M is the thickness of the confined aquifer [L]; S is the elastic drainable porosity of the confined aquifer, which can be expressed as $S = S_s M$, for which S_s is the specific storage [L^{-1}]; t is time [T]; Q is the constant pumping rate [$L^3 T^{-1}$].

A cylindrical coordinate system is established with the origin located at the intersection of the well center axis and the bottom of the shallow aquifer. The governing equations for groundwater flow in the shallow aquifer under cylindrical coordinates can be expressed as:

$$h \frac{\partial^2 h}{\partial r^2} + \frac{h}{r} \frac{\partial h}{\partial r} - \frac{K_v}{K_1} (i - i_0) = \frac{\mu_d}{K_1} \frac{\partial h}{\partial t} \quad (i > i_0) \quad (7)$$

$$h \frac{\partial^2 h}{\partial r^2} + \frac{h}{r} \frac{\partial h}{\partial r} = \frac{\mu_d}{K_1} \frac{\partial h}{\partial t} \quad (i \leq i_0) \quad (8)$$

$$h(r, 0) = h_0 \quad (9)$$

$$\frac{\partial h}{\partial r} (r \rightarrow r_w, t) = 0 \quad (10)$$

$$h(r \rightarrow +\infty, t) = h_0 \quad (11)$$

where h is the head of phreatic groundwater [L]; K_1 represents the hydraulic conductivity of the shallow aquifer [$L T^{-1}$]; μ_d is the specific yield of the shallow aquifer; i is the vertical hydraulic gradient, which can be expressed as $i = (h + m + M - H)/m$; m is the thickness of the aquitard [L]; h_0 is the initial head of the phreatic groundwater [L], which can be expressed as $h_0 = H_0 - (m + M)$.

Numerical solutions

Due to the non-Darcian flow in the aquitard, it is difficult to obtain analytical solutions; therefore, the finite

difference method is employed to solve this model. To improve computational efficiency, finer grid spaces are needed near the pumping well where the groundwater head changes greatly and coarser grid spaces are needed far away from the well where the changes are gentler. In this study, the nonuniform mesh generation method is adopted to discretize the radial axis into N nodes (Mathias et al. 2008; Wang et al. 2017). The distance of each node from the pumping well is expressed as:

$$r_j = (r_{j-1/2} + r_{j+1/2})/2 \quad j = 1 \dots N \quad (12)$$

in which

$$\log_{10}(r_{j+1/2}) = \log_{10}(r_w) + j \left[\frac{\log_{10}(r_e) - \log_{10}(r_w)}{N} \right] \quad j = 0 \dots N \quad (13)$$

where N is the total number of nodes; r_e is a large radial distance from the well indicating the infinite boundary.

With the aforementioned nonuniform mesh generation method, the governing Eq. (2) for groundwater flow in the confined aquifer can be discretized in space as follows:

$$A_{y1} H_{j-1}^{n+1} + B_{y1} H_j^{n+1} + C_{y1} H_{j+1}^{n+1} + D_{y1} H_j^{n+1} = E_{y1} + F_{y1} H_j^n \quad (14)$$

in which

$$A_{y1} = \frac{1}{(r_{j+1/2} - r_{j-1/2})(r_j - r_{j-1})},$$

$$B_{y1} = -\frac{1}{(r_{j+1/2} - r_{j-1/2})(r_{j+1} - r_j)} - \frac{1}{(r_{j+1/2} - r_{j-1/2})(r_j - r_{j-1})} - \frac{1}{r_j(r_{j+1} - r_j)} - \frac{K_v}{Tm} - \frac{S}{T\Delta t},$$

$$C_{y1} = \frac{1}{(r_{j+1/2} - r_{j-1/2})(r_{j+1} - r_j)} + \frac{1}{r_j(r_{j+1} - r_j)},$$

$$D_{y1} = \frac{K_v}{Tm}, E_{y1} = \frac{i_0 K_v}{T} - \frac{K_v(m+M_0)}{Tm}, \text{ and } F_{y1} = -\frac{S}{T\Delta t}$$

Equation (3) for the nonleaky zone in the confined aquifer can be expressed as:

$$A_{w1} H_{j-1}^{n+1} + B_{w1} H_j^{n+1} + C_{w1} H_{j+1}^{n+1} = D_{w1} H_j^n \quad (15)$$

in which

$$A_{w1} = \frac{1}{(r_{j+1/2} - r_{j-1/2})(r_j - r_{j-1})},$$

$$B_{w1} = -\frac{1}{(r_{j+1/2} - r_{j-1/2})(r_{j+1} - r_j)} - \frac{1}{(r_{j+1/2} - r_{j-1/2})(r_j - r_{j-1})} - \frac{1}{r_j(r_{j+1} - r_j)} - \frac{S}{T\Delta t},$$

$$C_{w1} = \frac{1}{(r_{j+1/2} - r_{j-1/2})(r_{j+1} - r_j)} + \frac{1}{r_j(r_{j+1} - r_j)}, \text{ and } D_{w1} = -\frac{S}{T\Delta t}.$$

Equation (7) can be expressed as

$$A_{y2} h_{j-1}^{n+1} + B_{y2} h_j^{n+1} + C_{y2} h_{j+1}^{n+1} + D_{y2} h_j^{n+1} = E_{y2} + F_{y2} h_j^n \quad (16)$$

Table 1 The default values for hydraulic parameters

Parameter	K_1 (m/day)	K_v (m/day)	Q (m ³ /day)	S	μ_d	T (m ² /day)
Value	5	0.0001	1,000	0.0001	0.15	250

in which

$$A_{y2} = \frac{h_j^n}{(r_{j+1/2} - r_{j-1/2})(r_j - r_{j-1})},$$

$$B_{y2} = -\frac{h_j^n}{(r_{j+1/2} - r_{j-1/2})(r_{j+1} - r_j)} - \frac{h_j^n}{(r_{j+1/2} - r_{j-1/2})(r_j - r_{j-1})}$$

$$- \frac{h_j^n}{r_j(r_{j+1} - r_j)} - \frac{K_v}{K_1 m} - \frac{\mu_d}{K_1 \Delta t},$$

$$C_{y2} = \frac{h_j^n}{(r_{j+1/2} - r_{j-1/2})(r_{j+1} - r_j)} + \frac{h_j^n}{r_j(r_{j+1} - r_j)},$$

$$D_{y2} = \frac{K_v}{K_1 m}, E_{y2} = \frac{K_v(m+M)}{K_1 m} - \frac{i_0 K_v}{K_1}, \text{ and } F_{y2} = -\frac{\mu_d}{K_1 \Delta t}$$

Equation (8) can be expressed as:

$$A_{w2} h_{j-1}^{n+1} + B_{w2} h_j^{n+1} + C_{w2} h_{j+1}^{n+1} = D_{w2} h_j^n \tag{17}$$

in which

$$A_{w2} = \frac{h_j^n}{(r_{j+1/2} - r_{j-1/2})(r_j - r_{j-1})},$$

$$B_{w2} = -\frac{h_j^n}{(r_{j+1/2} - r_{j-1/2})(r_{j+1} - r_j)} - \frac{h_j^n}{(r_{j+1/2} - r_{j-1/2})(r_j - r_{j-1})} - \frac{h_j^n}{r_j(r_{j+1} - r_j)} - \frac{\mu_d}{K_1 \Delta t},$$

$$C_{w2} = \frac{h_j^n}{(r_{j+1/2} - r_{j-1/2})(r_{j+1} - r_j)} + \frac{h_j^n}{r_j(r_{j+1} - r_j)}, \text{ and } D_{w2} = -\frac{\mu_d}{K_1 \Delta t}$$

By solving Eqs. (14)–(17) using MATLAB (Radha and Singh 2023), the distribution of groundwater heads in shallow and confined aquifers can be obtained. As the computational accuracy is significantly influenced by the time step, the iterative method is used to control the numerical error below some specified tolerance.

Results and discussion

In the following section, the impact of low-velocity non-Darcian flow on the movement of groundwater in a leaky aquifer system will be investigated under the condition of a well fully penetrating a confined aquifer. Both shallow and confined groundwater heads before pumping are assumed to be 100 m. The case being considered is that the thicknesses of the aquitard and confined aquifer are 5 and 50 m, respectively (Han et al. 2021; Yang et al. 2022). The default values for hydraulic parameters used in the study are shown in Table 1 (Shao et al. 2013; Zhang et al. 2015; Sun et al. 2016; Ma et al. 2017; Cheng et al. 2021). Then the results obtained from Darcian

and non-Darcian flows are compared under different influencing factors. The absolute error is used to reflect the difference between them and can be written as:

$$\Delta Y = Y_1 - Y_2 \tag{18}$$

where Y_1 and Y_2 are physical quantities obtained from Darcian and non-Darcian flow theories, respectively.

Impact of low-velocity non-Darcian flow on flow movement under different thicknesses of the aquitard

Based on extensive data collected through sample surveys, it is found that the thicknesses of aquitards in the North China Plain range mainly from 5 to 20 m (Zhan et al. 2014; Kwong et al. 2015; Han et al. 2021; Yang et al. 2022). To further investigate the relationship between the threshold pressure gradient of the aquitard and the distance of the dividing point from the pumping well, data for aquitard thicknesses of 5, 8, 11, 14, and 17 m under pseudo-steady-state conditions are plotted in Fig. 2. Due to the adoption of transient groundwater flow modeling, as pumping begins, the water head decreases, and the groundwater depression cone continuously expands. With the ongoing pumping, the rate of expansion of the groundwater depression cone gradually decreases. In the later stages of pumping, the temporal changes in groundwater head induced by the pumping become increasingly insignificant and can be considered negligible. This condition is referred to as a pseudo-steady-state condition. In this study, a criterion for determining the pseudo-steady-state condition is set, considering a water head difference less than 10^{-4} m between adjacent time steps. The other hydraulic parameters used are the same as those shown in Table 1. The results show that as the threshold pressure gradient of the aquitard increases, the distance between the dividing point of leaky and nonleaky areas and the pumping well decreases rapidly. This suggests that the hydraulic connection between shallow and confined aquifers is significantly weakened by the threshold pressure gradient of the aquitard, thereby reducing the vulnerability of the confined aquifer to salinization. In other words, the Darcian flow may lead to a significant overestimation of the leaky flow rate compared to the actual situation (non-Darcian flow). When the threshold pressure gradient of the aquitard is large enough, there will be no leakage between the

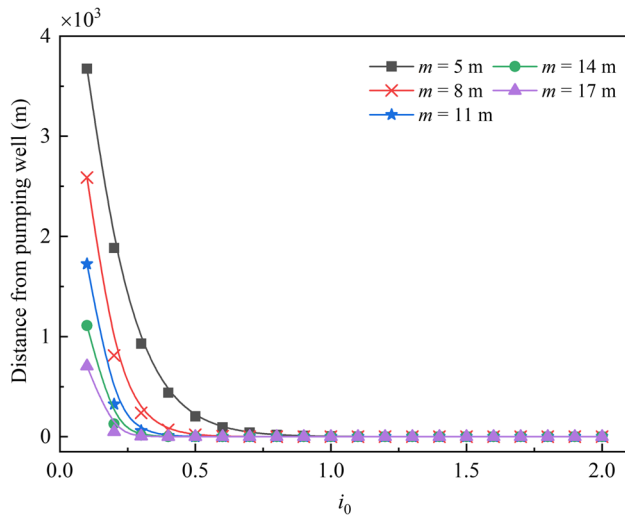


Fig. 2 The relationship between the threshold pressure gradient of the aquitard and the distance of the dividing point from the pumping well with different thicknesses of the aquitard (m in meters) under pseudo-steady-state conditions

shallow and confined aquifers; furthermore, the distance of the dividing point from the pumping well decreases as the aquitard thickness increases. Leaky areas in the aquifer system with a thicker aquitard are found to be less sensitive to the threshold pressure gradient of the aquitard when compared to systems with a thinner aquitard, which can be explained by the fact that the increase in aquitard thickness reduces the vertical hydraulic gradient in the aquitard, resulting in a smaller leaky area.

To further examine the relationship between the intensity of leakage and the threshold pressure gradient of the aquitard, the characteristics of the vertical flow velocities in the aquitard near the pumping well under different thicknesses of the aquitard are analyzed, as they represent the maximum vertical flow velocities in the leaky aquifer system. Figure 3 illustrates the variation of the vertical flow velocity in the aquitard near the pumping well for different thicknesses of the aquitard under pseudo-steady-state conditions with the threshold pressure gradient of the aquitard. It can be observed that, as the threshold pressure gradient increases, the vertical flow velocity decreases to zero and then remains stable. The slopes of all these curves at the decreasing stage are nearly the same and approximately linear, due to the fact that the flux-gradient relationship used in Eq. (1) is linear and the vertical hydraulic conductivity of the aquitard remains identical. The slight nonlinearity might arise from the fact that variations in the threshold pressure gradient can

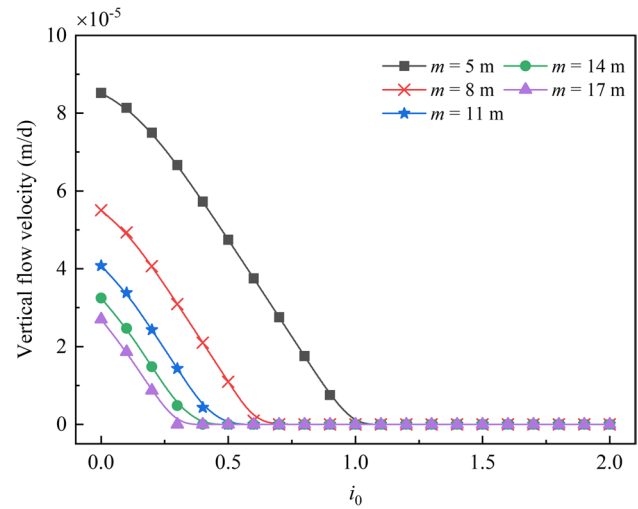


Fig. 3 The variation of the vertical flow velocity in the aquitard near the pumping well for different thicknesses of the aquitard (m) under pseudo-steady-state conditions with the threshold pressure gradient of the aquitard

influence the drawdown curve during a pseudo steady state. This, in turn, affects the vertical hydraulic gradient and ultimately impacts the final vertical velocity within the aquitard. In the case of a thick aquitard, the vertical flow velocity is significantly reduced, and the rate of decrease becomes gradually smaller. Figure 4 shows the absolute error of the vertical flow velocity in the aquitard calculated using Eq. (18). The results indicate that the differences between the results calculated from Darcian and non-Darcian flows increase with an increase in the threshold pressure gradient in the aquitard. This difference is positively correlated with the thickness of the aquitard under a small threshold pressure gradient, and negatively correlated with the thickness of the aquitard under a large threshold pressure gradient, which is to be expected. When i_0 is extremely small, the water flow within the aquitard approximates Darcian flow. During this scenario, the impact of non-Darcian flow becomes more pronounced only when the aquitard is considerably thick. Conversely, when i_0 is significantly large, the entire region has transitioned into a nonleaky area. In this scenario, the disparity in vertical flow velocity between Darcian and non-Darcian flows equals the vertical flow velocity observed under Darcian flow conditions. As the thickness of the aquitard increases, the vertical flow velocity in the aquitard decreases. Based on the above analysis, for a leaky aquifer system with a thinner aquitard under a substantial threshold pressure gradient, the assessment method based on Darcy's law may lead to a

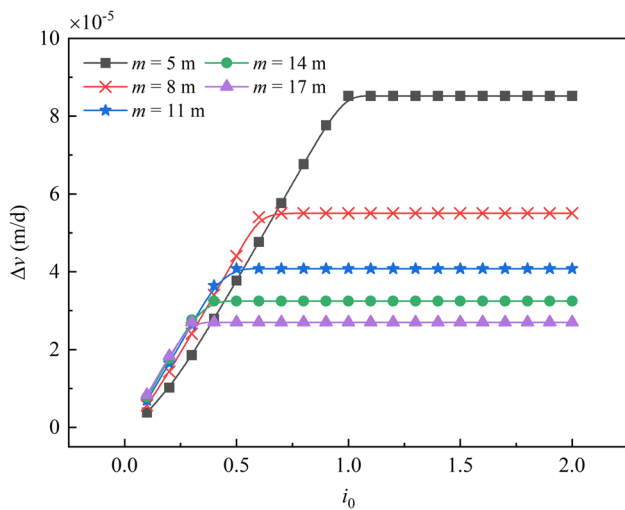


Fig. 4 The difference between the vertical flow velocities in the aquitard calculated from Darcian and non-Darcian flows under different thicknesses of the aquitard (m)

significant overestimation of both the leaky flow rate and the potential risk of salination.

Impact of low-velocity non-Darcian flow on flow movement under different pumping rates

Figure 5 illustrates the impact of low-velocity non-Darcian flow on flow movement under different pumping rates. The pumping rates considered are 400, 800, 1,200, 1,600, and 2,000 m^3/day , respectively. The other hydraulic parameters

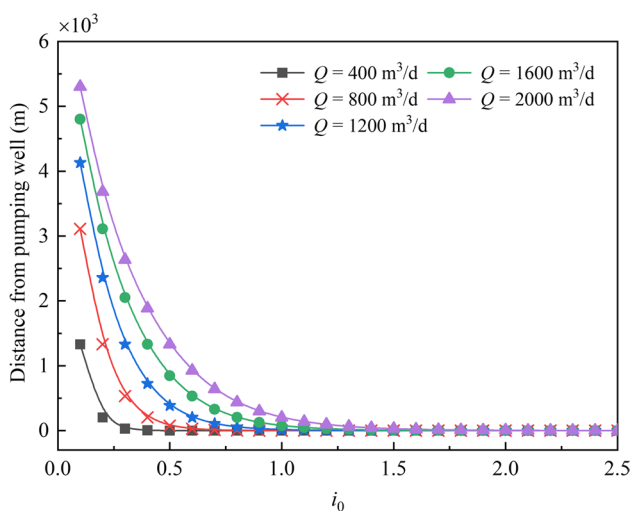


Fig. 5 The relationship between the threshold pressure gradient of the aquitard and the distance of the dividing point from the pumping well with different pumping rates (Q) under pseudo-steady-state conditions

are the same as shown in Table 1. It can be observed that the leaky area reduces rapidly with an increase in the threshold pressure gradient of the aquitard, and this trend becomes more pronounced with an increase in the pumping rate. The leaky area is positively correlated with the pumping rate, and the difference in leaky areas under different pumping rates decreases with an increase in the threshold pressure gradient of the aquitard. Therefore, in a leaky aquifer system experiencing significant exploitation from the confined aquifer, there is a considerable risk of overestimating both the leaky flow rate and the potential for salination if non-Darcian flow is disregarded.

Figure 6 illustrates the variation of the vertical flow velocity in the aquitard near the pumping well for different pumping rates under pseudo-steady-state conditions with the threshold pressure gradient of the aquitard. It indicates that, after a sort of warm-up period, the vertical flow velocity linearly decreases with the increase of the threshold pressure gradient, and all of these curves have the same slope at the decreasing stage. This explanation is the same as that in section ‘Impact of low-velocity non-Darcian flow on flow movement under different thicknesses of the aquitard’. In particular, the slight non-linearity may be due to the fact that the pumping rate can impact the drawdown curve under pseudo-steady-state and further affect the final vertical velocity in the aquitard. Additionally, because, under pseudo-steady-state conditions, the pumping rate near the well is primarily supplied by leaky recharge from the shallow aquifer, the adjacent curves are distributed at almost equally spaced intervals. Figure 7 displays the absolute error of the vertical flow velocity in the aquitard calculated from Eq. (18). The differences between the results obtained from

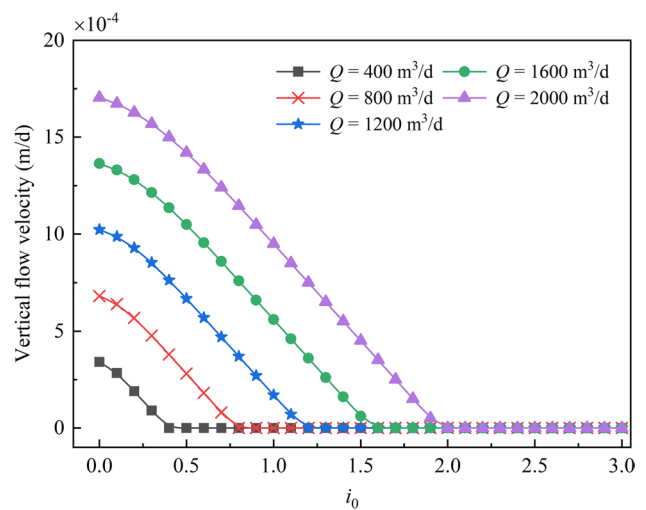


Fig. 6 The variation of the vertical flow velocity in the aquitard near the pumping well for different pumping rates (Q) under pseudo-steady-state conditions with the threshold pressure gradient of the aquitard

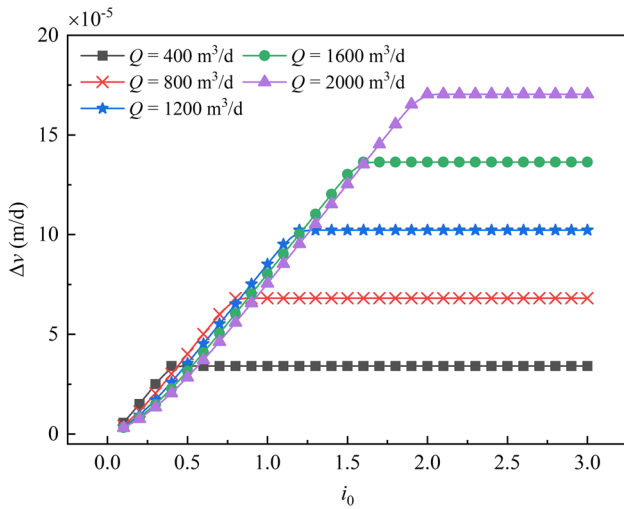


Fig. 7 The difference between the vertical flow velocities in the aquitard calculated from Darcian and non-Darcian flows under different pumping rates (Q)

Darcian and non-Darcian flows increase with the increase of the threshold pressure gradient in the aquitard. This difference is negatively correlated with the pumping rate under small threshold pressure gradients and positively correlated with the pumping rate under large threshold pressure gradients.

Impact of low-velocity non-Darcian flow on flow movement under different transmissivity values for the confined aquifer

Figure 8 shows the impact of low-velocity non-Darcian flow on flow movement with different values of

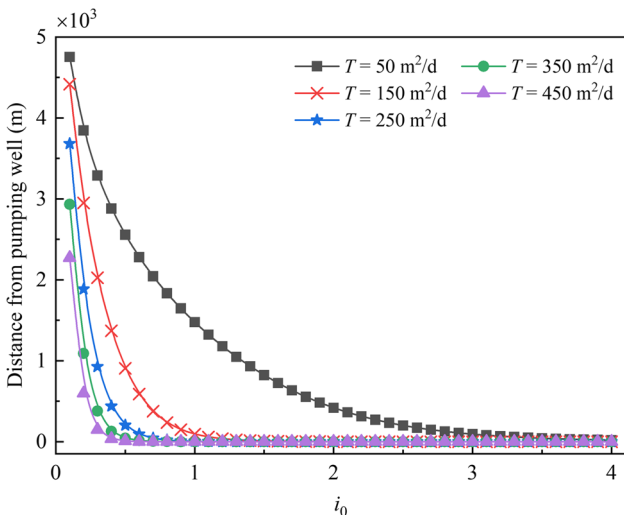


Fig. 8 The relationship between the threshold pressure gradient of the aquitard and the distance of the dividing point from the pumping well with different transmissivity (T) values for the confined aquifer under pseudo-steady-state conditions

transmissivity for the confined aquifer: $T = 50, 150, 250, 350,$ and $450 \text{ m}^2/\text{day}$. The other hydraulic parameters are the same as shown in Table 1. The results indicate that the leaky area reduces rapidly with the increase of the threshold pressure gradient of the aquitard and this trend becomes more pronounced with the increase in transmissivity. The leaky area is negatively correlated with the transmissivity value, and the difference in leaky areas under different transmissivity values first increases and then decreases with the increase of the threshold pressure gradient of the aquitard, which is to be expected. Compared with no threshold pressure gradient of the aquitard, the drawdown of the confined groundwater head is extended under a small threshold pressure gradient of the aquitard leading to an increase in the leaky area. With the threshold pressure gradient of the aquitard further increasing, leakage becomes more and more difficult. This result implies that the threshold pressure gradient can have a significant impact on the extent of leakage, subsequently reducing the risk of salination in the confined aquifer.

Figure 9 shows the variation of the vertical flow velocity in the aquitard near the pumping well for different transmissivity values under pseudo-steady-state conditions with the threshold pressure gradient of the aquitard. This figure illustrates that the vertical flow velocity decreases with the increase of the threshold pressure gradient, and the spaced intervals between adjacent curves vary greatly. The vertical flow velocity in the aquitard increases rapidly with the decrease in transmissivity. The absolute error of the vertical flow velocity in the aquitard calculated from Eq. (18) is displayed in Fig. 10. As the threshold pressure gradient

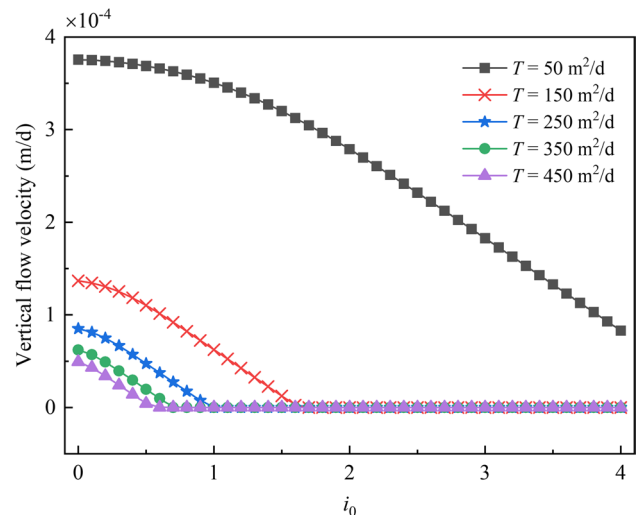


Fig. 9 The variation of the vertical flow velocity in the aquitard near the pumping well for different transmissivity (T) values under pseudo-steady-state conditions with the threshold pressure gradient of the aquitard

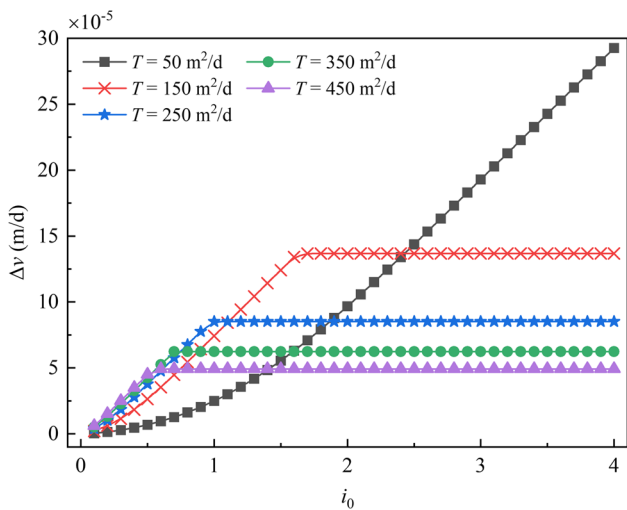


Fig. 10 The difference between vertical flow velocities in the aquitard calculated from Darcian and non-Darcian flows under different transmissivity (T) values for the confined aquifer

in the aquitard increases, the differences between the results calculated from Darcian and non-Darcian flows increase, and the error curves change from concave to approximately linear with the increase in transmissivity. The explanation is as follows: When the transmissivity for the confined aquifer is extremely small, the lateral recharge capacity of the confined aquifer is notably low. The drawdown of the confined groundwater head near the pumping well is extremely significant, while a significant hydraulic head disparity exists between the unconfined and confined aquifers. Consequently, a substantial vertical hydraulic gradient develops within the aquitard. In this context, minor fluctuations in i_0 , when it is at a very small value, minimally impact the vertical flow velocity within the aquitard; however, as i_0 progressively increases, its influence becomes progressively more conspicuous, leading to the emergence of a concave curve in situations where the transmissivity for the confined aquifer is very small. Especially for small transmissivity values (like an aquifer of fine sand), the absolute error of the vertical flow velocity in the aquitard is significant under a large threshold pressure gradient in the aquitard (like clay layer or shale layer), which should be given more attention and one should consider the impact of non-Darcian flow.

Impact of low-velocity non-Darcian flow on flow movement under different leaky coefficients

The leaky coefficient is expressed as

$$\sigma = \frac{K_v}{m} \tag{19}$$

The following paragraphs discuss five sets of leaky coefficients: 8.0×10^{-6} , 1.6×10^{-5} , 2.4×10^{-5} , 3.2×10^{-5} , and 4.0×10^{-5} /day. The other hydraulic parameters remain the same as shown in Table 1. Figure 11 illustrates the relationship between the threshold pressure gradient of the aquitard and the distance of the dividing point from the pumping well with different leaky coefficients under pseudo-steady-state conditions. This figure suggests that the leaky area decreases rapidly with the increase of the threshold pressure gradient of the aquitard, and the leaky area is negatively correlated with the leaky coefficient. For a small threshold pressure gradient of the aquitard, the difference of the leaky area between different leaky coefficients is significant; however, with the increase of the threshold pressure gradient of the aquitard, this difference quickly disappears.

Figure 12 shows the variation of the vertical flow velocity in the aquitard near the pumping well for different leaky coefficients under pseudo-steady-state conditions with the threshold pressure gradient of the aquitard. Meanwhile, Fig. 13 displays the absolute error of the vertical flow velocity in the aquitard calculated from Eq. (18). Three observations can be made from these figures. Firstly, the vertical flow velocity and the spaced intervals between adjacent curves decrease with the increase of the threshold pressure gradient. Secondly, the vertical flow velocity is positively correlated with

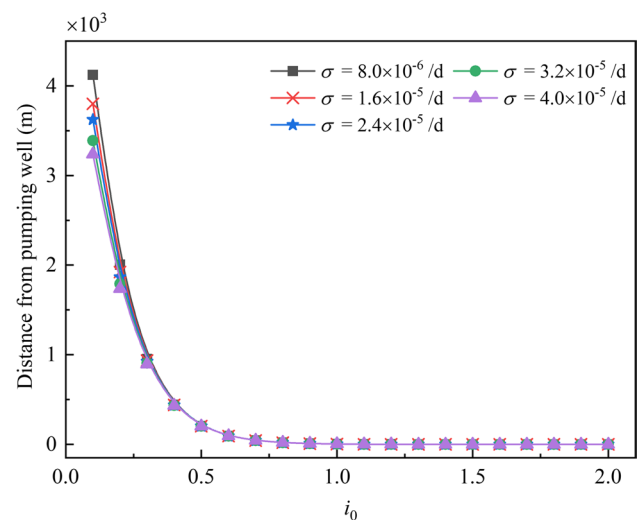


Fig. 11 The relationship between the threshold pressure gradient of the aquitard and the distance of the dividing point from the pumping well with different leaky coefficients (σ) under pseudo-steady-state conditions

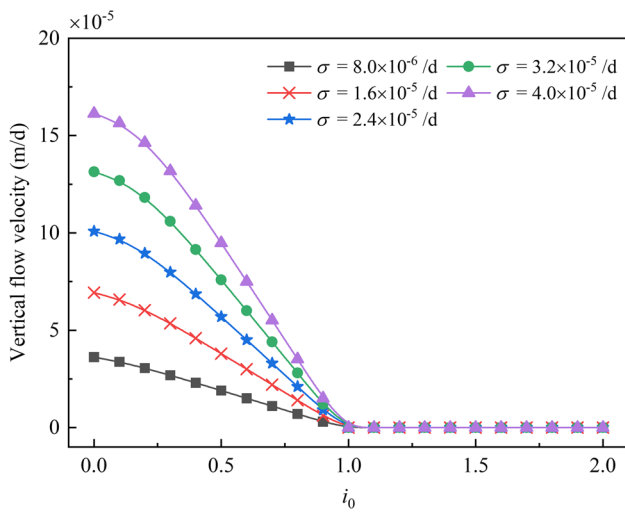


Fig. 12 The variation of the vertical flow velocity in the aquitard near the pumping well for different leaky coefficients (σ) under pseudo-steady-state conditions with the threshold pressure gradient of the aquitard

the leaky coefficient, while thirdly, with the increase of the threshold pressure gradient in the aquitard, the differences between the results calculated from Darcian and non-Darcian flows increase, and a large leaky coefficient increases this difference.

Figure 12 illustrates that when $i_0 > 1.0$, the vertical flow velocity in the aquitard is reduced to 0. Conversely, when $i_0 < 1.0$, an increase in the threshold pressure gradient corresponds to a diminishing vertical flow velocity. The underlying reasons for this observed behavior can be elucidated as follows. The threshold pressure gradient for non-Darcian flow can result in the emergence of a non-leaky area when the vertical hydraulic gradient falls within

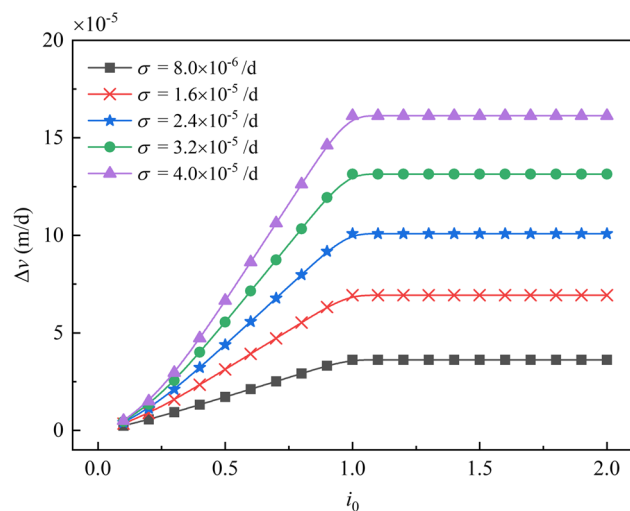


Fig. 13 The difference between vertical flow velocities in the aquitard calculated from Darcian and non-Darcian flows under different leaky coefficients (σ)

the range of $0 < i < i_0$. Two factors, namely the pumping rate and the threshold pressure gradient, can influence the distance between the pumping well and the starting point of the nonleaky area. Additionally, the vertical hydraulic conductivity value of the aquitard only affects the vertical flow velocity within the leaky area. Figure 12 illustrates the variation of the vertical flow velocity in the aquitard near the pumping well ($r = 5$ m). As the value of i_0 increases, the distance between the pumping well and the starting point of the nonleaky area becomes progressively smaller. When $i_0 = 1.0$, the separation point between the leaky and nonleaky areas occurs at $r = 5$ m; consequently, all curves approach zero when $i_0 > 1.0$. Within the leaky area, a higher vertical hydraulic conductivity of the aquitard and a smaller i_0 result in a larger vertical flow velocity in the aquitard.

Impact of low-velocity non-Darcian flow on flow movement under different values of elastic drainable porosity

The impact of low-velocity non-Darcian flow on flow movement is shown in Fig. 14 for different values of elastic drainable porosity, $S = 1.0 \times 10^{-5}$, $S = 5.0 \times 10^{-5}$, $S = 1.0 \times 10^{-4}$, $S = 1.5 \times 10^{-4}$, $S = 2.0 \times 10^{-4}$. Figure 15 illustrates the variation of the vertical flow velocity in the aquitard near the pumping well for different values of elastic drainable porosity under pseudo-steady-state conditions with the threshold pressure gradient of the aquitard. The absolute error of the vertical flow velocity in the aquitard calculated from Eq. (18) is shown in Fig. 16. The other hydraulic parameters are the same

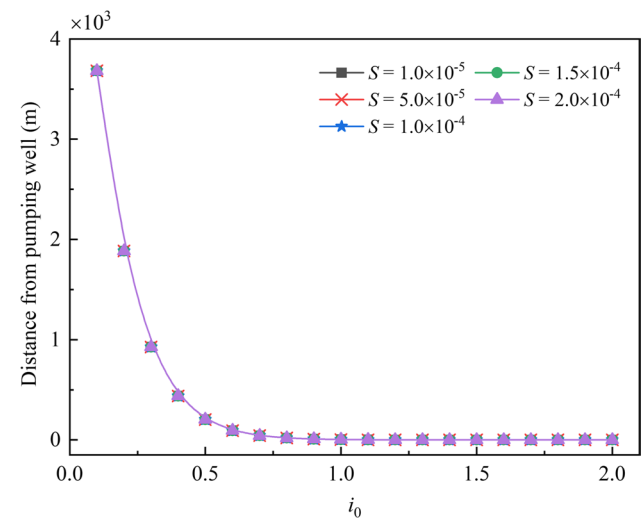


Fig. 14 The relationship between the threshold pressure gradient of the aquitard and the distance of the dividing point from the pumping well with different elastic drainable porosity (S) values under pseudo-steady-state conditions

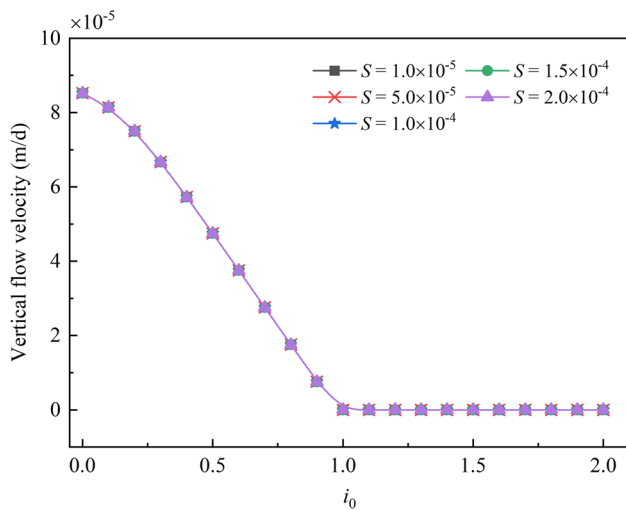


Fig. 15 The variation of the vertical flow velocity in the aquitard near the pumping well for different values of elastic drainable porosity (S) under pseudo-steady-state conditions with the threshold pressure gradient of the aquitard

as shown in Table 1. In addition to the impact of the threshold pressure gradient of the aquitard on the leaky area and vertical flow velocity discussed in the first four subsections of section ‘Results and discussion, it can be observed from Figs. 14, 15 and 16 that there is no obvious impact of elastic drainable porosity on the leaky area and vertical flow velocity in the aquitard under pseudo-steady-state conditions. This can be explained by considering a vertically cylindrical domain of confined aquifer surrounding the well. The total pumping rate is composed of water released from the confined aquifer storage within that cylinder, influx outside that

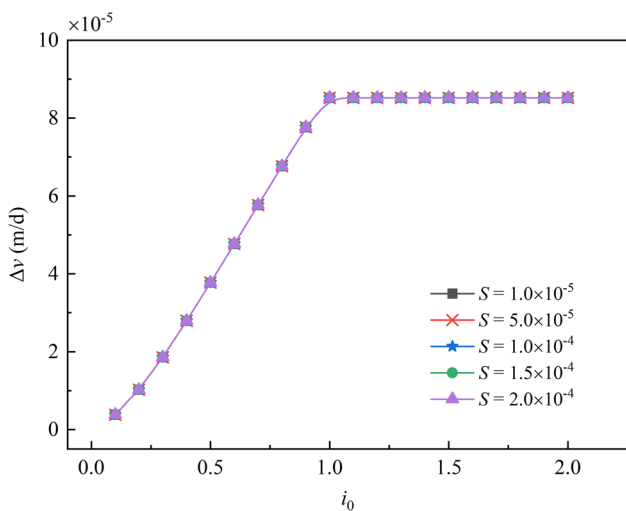


Fig. 16 The difference of the vertical flow velocity in the aquitard calculated from Darcian and non-Darcian flows under different values of elastic drainable porosity (S)

cylinder, and the leaky recharge from the shallow aquifer; therefore, elastic drainable porosity mainly controls the variation of groundwater head and has little effect on the final state.

Impact of low-velocity non-Darcian flow on flow movement under different hydrogeological parameters of the shallow aquifer

The impact of low-velocity non-Darcian flow on flow movement under different hydrogeological parameters of the shallow aquifer is depicted in Fig. 17. The other hydraulic parameters are the same as shown in Table 1. Figure 18 displays the variation of the vertical flow velocity in the aquitard near the pumping well

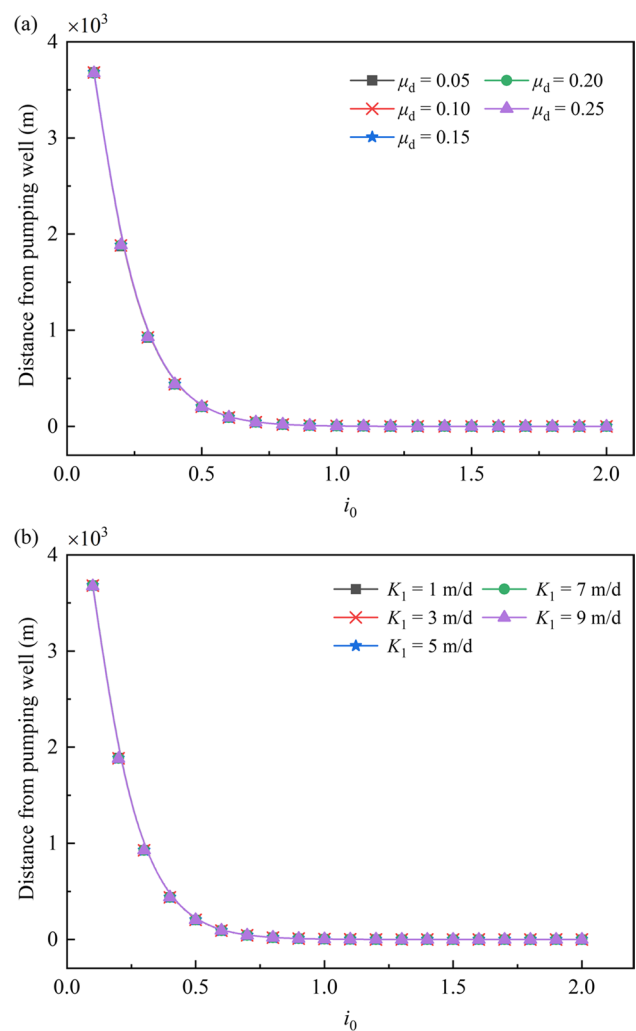


Fig. 17 The relationship between the threshold pressure gradient of the aquitard and the distance of the dividing point from the pumping well with different hydrogeological parameters of the shallow aquifer (a the specific yield of the shallow aquifer, μ_d ; b the hydraulic conductivity of the shallow aquifer, K_1) under pseudo-steady-state conditions

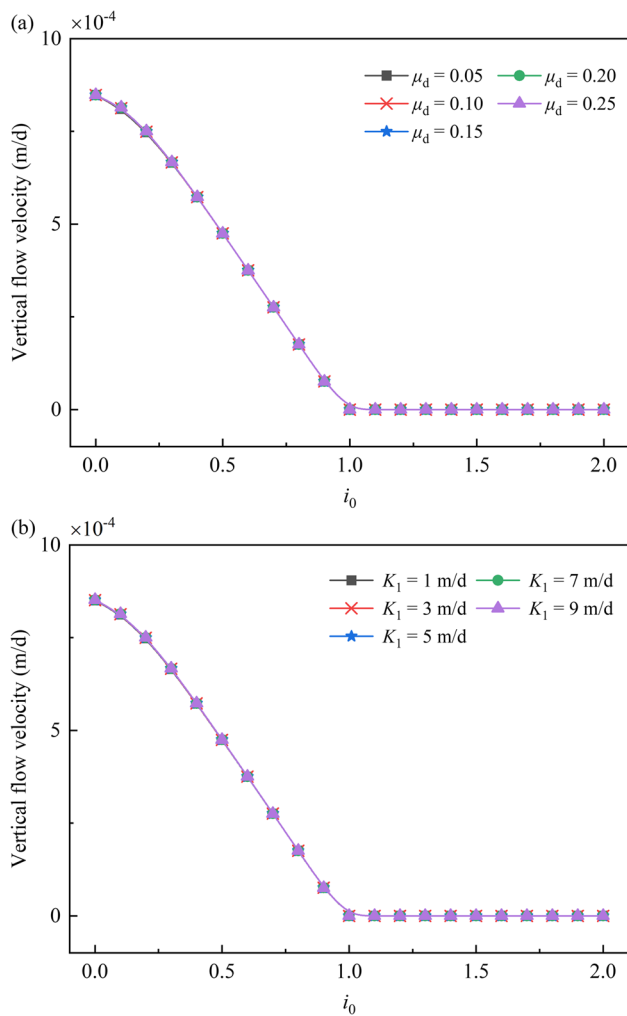


Fig. 18 The variation of the vertical flow velocity in the aquitard near the pumping well for various hydrogeological parameters of the shallow aquifer (**a** the specific yield of the shallow aquifer, μ_d ; **b** the hydraulic conductivity of the shallow aquifer, K_1) under pseudo-steady-state conditions with the threshold pressure gradient of the aquitard

for various hydrogeological parameters of the shallow aquifer under pseudo-steady-state conditions with the threshold pressure gradient of the aquitard. Figure 19 illustrates the absolute error of the vertical flow velocity in the aquitard calculated using Eq. (18). It can be observed from these figures that the hydrogeological parameters of the shallow aquifer have little effect on the leaky area and vertical flow velocity in the aquitard under pseudo-steady-state conditions, in addition to the impact of the threshold pressure gradient of the aquitard mentioned in the first four subsections of section ‘Results and discussion’. This finding can be explained similarly to what is discussed in section ‘Impact of low-velocity non-Darcian flow on flow movement under different values of elastic drainable porosity’.

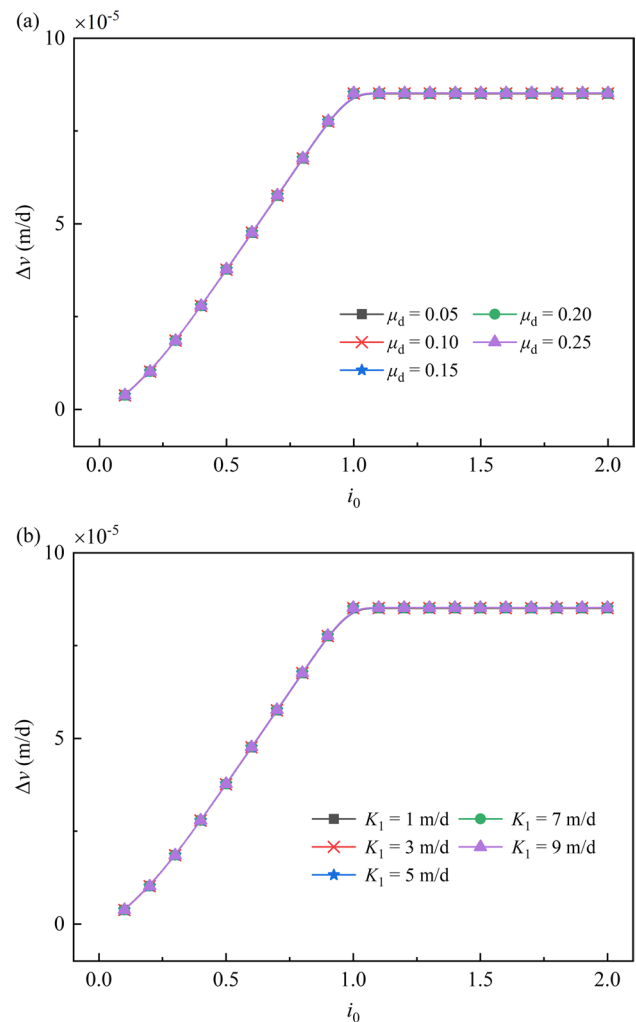


Fig. 19 The difference between vertical flow velocities in the aquitard calculated from Darcian and non-Darcian flows under different hydrogeological parameters of the shallow aquifer (**a** the specific yield of the shallow aquifer, μ_d ; **b** the hydraulic conductivity of the shallow aquifer, K_1)

Summary and conclusions

According to traditional groundwater seepage theory, known as Darcy’s law, the shallow groundwater in the North China Plain should have entered the confined aquifer over a large area due to a significant head difference. Considering the substantial contamination or salinity present in a significant portion of shallow groundwater, this leakage was anticipated to exert a significant influence on the water quality of the deep confined aquifer; however, in reality, there is no apparent salinization of the deep groundwater. This paper aims to explain this phenomenon based on the seepage characteristics of low-permeability media. A finite difference method is employed to solve for low-velocity

non-Darcian flow to a well that fully penetrates a confined aquifer. In this model, the flows in both shallow and confined aquifers are assumed to be Darcian and horizontal, while leakage through the aquitard is assumed to be non-Darcian and vertical. The study investigates the effect of low-velocity non-Darcian flow in the aquitard on the groundwater flow in the leaky aquifer system and analyzes the difference between Darcian and non-Darcian flows. The following conclusions can be drawn from this study.

1. Low-velocity non-Darcian flow in the aquitard considerably slows down the leakage from the shallow aquifer. The leakage area and vertical flow velocity are weakened by the threshold pressure gradient. As a result, the assessment method relying on Darcy's law would lead to a considerable overestimation of both the leakage and the risk of salination in the confined aquifer.
2. The vertical flow velocity in the aquitard near the pumping well decreases with the increase of the threshold pressure gradient. The non-Darcian vertical flow velocity is significantly lower than that obtained from Darcian theory. These findings offer mechanistic evidence for the overestimation of leakage and the associated risk of salination in the confined aquifer due to the oversight of non-Darcian flow.
3. The difference between the vertical flow velocity in the aquitard calculated from Darcian and non-Darcian flows is significant under the situation of a thin aquitard thickness, large pumping rate, small transmissivity, and a large leaky coefficient when the threshold pressure gradient is large. Under the aforementioned conditions, disregarding non-Darcian flow could lead to a significant overestimation of the salination risk in the confined aquifer within the North China Plain.

The findings of this study offer important insights into why the confined aquifer in the North China Plain has not experienced significant salination despite the influence of distributed depression cones, particularly from the perspective of non-Darcian flow. Moreover, given the widespread occurrence of leaky aquifer systems around the world, these findings hold valuable implications for groundwater issues in regions sharing similar characteristics. However, several limitations exist within this study's findings—the numerical model, for instance, does not incorporate the effects of chemical reactions, nonequilibrium adsorption, and dispersion in solute transport. These aspects will be addressed in future studies.

Funding This research was supported by National Natural Science Foundation of China (51979252, 52279025) and China Scholarship Council (CSC) (202106415007).

Declarations

Conflict of interest The authors declare no conflict of interest.

References

- Cai JC (2014) A fractal approach to low velocity non-Darcy flow in a low permeability porous medium. *Chin Phys B* 23(4):044701. <https://doi.org/10.1088/1674-1056/23/4/044701>
- Cao G, Han D, Currell MJ, Zheng C (2016) Revised conceptualization of the North China Basin groundwater flow system: groundwater age, heat and flow simulations. *J Asian Earth Sci* 127:119–136. <https://doi.org/10.1016/j.jseas.2016.05.025>
- Cao GL (2013) Evaluation of groundwater system in the North China plain using groundwater modeling. PhD Thesis, China University of Geosciences, Beijing, China
- Chen C (2019) A continuum-scale two-parameter model for non-Darcian flow in low-permeability porous media. *Hydrogeol J* 27(7):2637–2643. <https://doi.org/10.1007/s10040-019-02010-2>
- Chen JY (2010) Holistic assessment of groundwater resources and regional environmental problems in the North China plain. *Environ Earth Sci* 61(5):1037–1047. <https://doi.org/10.1007/s12665-009-0425-6>
- Chen JY, Tang CY, Shen YJ, Sakura Y, Kondoh A, Shimada J (2003) Use of water balance calculation and tritium to examine the drop-down of groundwater table in the piedmont of the North China plain (NCP). *Environ Geol* 44(5):564–571. <https://doi.org/10.1007/s00254-003-0792-3>
- Chen XZ, Wang PX, Muhammad T, Xu ZC, Li YK (2020) Subsystem-level groundwater footprint assessment in North China plain: the world's largest groundwater depression cone. *Ecol Indic* 117:106662. <https://doi.org/10.1016/j.ecolind.2020.106662>
- Cheng ZS, Su C, Zheng ZX, Chen ZY, Wei W (2021) Characterize groundwater vulnerability to intensive groundwater exploitation using tritium time-series and hydrochemical data in Shijiazhuang, North China plain. *J Hydrol* 603(B):126953. <https://doi.org/10.1016/j.jhydrol.2021.126953>
- Cui LH, Cheng JM, Lu WL, Li MM (2014) Numerical study on salt-water downward migration in aquitard as low velocity non-Darcy flow. *J Hydraul Eng* 45(7):875–882. <https://doi.org/10.13243/j.cnki.slxb.2014.07.015>
- Foster S, Garduno H, Evans R, Olson D, Tian Y, Zhang WZ, Han ZS (2004) Quaternary aquifer of the North China plain: assessing and achieving groundwater resource sustainability. *Hydrogeol J* 12(1):81–93. <https://doi.org/10.1007/s10040-003-0300-6>
- Han D, Cao G, Currell MJ, Priestley SC, Love AJ (2020) Groundwater salinization and flushing during glacial-interglacial cycles: insights from aquitard porewater tracer profiles in the North China plain. *Water Resour Res* 56(11):e2020WR027879. <https://doi.org/10.1029/2020WR027879>
- Han DM, Currell MJ, Guo HM (2021) Controls on distributions of sulphate, fluoride, and salinity in aquitard porewater from the North China plain: long-term implications for groundwater quality. *J Hydrol* 603(A):126828. <https://doi.org/10.1016/j.jhydrol.2021.126828>

- Hantush MS, Jacob CE (1955) Non-steady radial flow in an infinite leaky aquifer. *Trans Am Geophys Union* 36(1):95–100. <https://doi.org/10.1029/TR036i001p00095>
- Hu AF, Chen Y, Xie SL, Chen YY, Hou J (2022) Consolidation analysis for soft clay reinforced by a granular column with non-Darcian flow. *Int J Geomech* 22(10):04022166. [https://doi.org/10.1061/\(ASCE\)GM.1943-5622.0002507](https://doi.org/10.1061/(ASCE)GM.1943-5622.0002507)
- Jiang L, Bai L, Zhao Y, Cao G, Wang H, Sun Q (2018) Combining InSAR and hydraulic head measurements to estimate aquifer parameters and storage variations of confined aquifer system in Cangzhou North China plain. *Water Resour Res* 54(10):8234–8252. <https://doi.org/10.1029/2017WR022126>
- Kwong HT, Jiao JJ, Liu K, Guo HP, Yang SY (2015) Geochemical signature of pore water from core samples and its implications on the origin of saline pore water in Cangzhou, North China plain. *J Geochem Explor* 157:143–152. <https://doi.org/10.1016/j.gexplo.2015.06.008>
- Li CX, Xie KH, Hu AF, Hu BX (2012) One-dimensional consolidation of double-layered soil with non-Darcian flow described by exponent and threshold gradient. *J Cent South Univ* 19(2):562–571. <https://doi.org/10.1007/s11771-012-1040-3>
- Li J, Liang X, Jin MG, Mao XM (2013) Geochemical signature of aquitard pore water and its paleo-environment implications in Caofeidian Harbor, China. *Geochem J* 47(1):37–50. <https://doi.org/10.2343/geochemj.2.0238>
- Li S, Cheng JM, Li MM, Cui LH (2016) Water quality characteristics and evolution of groundwater system influenced by human exploitation activity in Hengshui area. *South-to-North Water Transf Water Sci Tech* 14(3):55–61. <https://doi.org/10.13476/j.cnki.nsbdkq.2016.03.010>
- Liu CM, Yu JJ, Kendy E (2001) Groundwater exploitation and its impact on the environment in the North China plain. *Water Int* 26(2):265–272. <https://doi.org/10.1080/02508060108686913>
- Liu F, Wang S, Yeh TCJ, Zhen PN, Wang LS, Shi LM (2020) Using multivariate statistical techniques and geochemical modelling to identify factors controlling the evolution of groundwater chemistry in a typical transitional area between Taihang Mountains and North China plain. *Hydrol Process* 34(8):888–1905. <https://doi.org/10.1002/hyp.13701>
- Liu HH, Birkholzer J (2012) On the relationship between water flux and hydraulic gradient for unsaturated and saturated clay. *J Hydrol* 475:242–247. <https://doi.org/10.1016/j.jhydrol.2012.09.057>
- Liu HH, Li LC, Birkholzer J (2012) Unsaturated properties for non-Darcian water flow in clay. *J Hydrol* 430–431:173–178. <https://doi.org/10.1016/j.jhydrol.2012.02.017>
- Liu K, Wen Z, Liang X, Pan HY, Liu JG (2013) One-dimensional column test for non-Darcy flow in low permeability media. *Chinese J Hydrol* 28(1):81–87. <https://doi.org/10.3969/j.issn1000-4874.2013.01.012>
- Luo E, Wang X, Hu Y, Wang J, Liu L (2019) Analytical solutions for non-Darcy transient flow with the threshold pressure gradient in multiple-porosity media. *Math Probl Eng* 2618254. <https://doi.org/10.1155/2019/2618254>
- Ma R, Shi JS, Shi XY (2017) Spatial variation of hydraulic conductivity categories in a highly heterogeneous aquifer: a case study in the North China plain (NCP). *J Earth Sci* 28(1):113–123. <https://doi.org/10.1007/s12583-016-0636-1>
- Mathias SA, Butler AP, Zhan H (2008) Approximate solutions for Forchheimer flow to a well. *J Hydraul Eng* 134(9):1318–1325. [https://doi.org/10.1061/\(ASCE\)0733-9429\(2008\)134:9\(1318\)](https://doi.org/10.1061/(ASCE)0733-9429(2008)134:9(1318))
- Meng XM, Shao JY, Yin MS, Liu DF, Xue XW (2015) Low velocity non-Darcian flow to a well fully penetrating a confined aquifer in the first kind of leaky aquifer system. *J Hydrol* 530:533–553. <https://doi.org/10.1016/j.jhydrol.2015.10.020>
- Nilson RH (1981) Transient fluid flow in porous media: inertia dominated to viscous dominated transition. *J Fluids Eng* 103(2):339–343. <https://doi.org/10.1115/1.3241743>
- Ophori DU (1998) Flow of groundwater with variable density and viscosity, Atikokan research area, Canada. *Hydrogeol J* 6(2):193–203. <https://doi.org/10.1007/s100400050144>
- Radha R, Singh MK (2023) Axial groundwater contaminant dispersion modeling for a finite heterogeneous porous medium. *Water* 15:2676. <https://doi.org/10.3390/w15142676>
- Shao JL, Li L, Cui YL, Zhang ZJ (2013) Groundwater flow simulation and its application in groundwater resource evaluation in the North China plain, China. *Acta Geol Sin* 87(1):243–253. <https://doi.org/10.1111/1755-6724.12045>
- Shi J, Zhao W, Zhang Z, Fei Y, Li Y, Zhang F, Chen J, Yong Q (2011) Assessment of deep groundwater over-exploitation in the North China plain. *Geosci Front* 2(4):593–598. <https://doi.org/10.1016/j.gsf.2011.07.002>
- Shi JS, Li GM, Liang X, Chen ZY, Shao JL, Song XF (2014) Evolution mechanism and control of groundwater in the North China plain. *Acta Geosci Sin* 35(5):527–534. <https://doi.org/10.3975/cagsb.2014.05.01>
- Shi MJ, Gao ZJ, Wan L, Guo HP, Zhang HY, Liu JT (2019) Desalination of saline groundwater by a weakly permeable clay stratum: a case study in the North China plain. *Environ Earth Sci* 78(17):547. <https://doi.org/10.1007/s12665-019-8558-8>
- Simmons C (2005) Variable density groundwater flow: from current challenges to future possibilities. *Hydrogeol J* 13:116–119. <https://doi.org/10.1007/s10040-004-0408-3>
- Su C, Cheng ZS, Wei W, Chen ZY (2018) Assessing groundwater availability and the response of the groundwater system to intensive exploitation in the North China plain by analysis of long-term isotopic tracer data. *Hydrogeol J* 26(5):1401–1415. <https://doi.org/10.1007/s10040-018-1761-y>
- Sun XM, Wu JF, Shi XQ, Wu JC (2016) Experimental and numerical modeling of chemical osmosis in the clay samples of the aquitard in the North China plain. *Environ Earth Sci* 75(1):59. <https://doi.org/10.1007/s12665-015-4921-6>
- Teng YT, Wang YF, Li ZH, Qiao R, Chen C (2023) Temperature effect on non-Darcian flow in low-permeability porous media. *J Hydrol* 616:128780. <https://doi.org/10.1016/j.jhydrol.2022.128780>
- Wang JB (2002) Leakage recharge from pores saline groundwater to deep fresh groundwater on the condition of pumping in Huabei plain: a case of Tianjing plain. *Hydrogeol Eng Geol* 6:35–37. <https://doi.org/10.16030/j.cnki.issn.1000-3665.2002.06.009>
- Wang QR, Zhan HB, Wang YX (2017) Single-well push-pull test in transient Forchheimer flow field. *J Hydrol* 549:125–132. <https://doi.org/10.1016/j.jhydrol.2017.03.066>
- Wang YX, Zheng CM, Ma R (2018) Review: Safe and sustainable groundwater supply in China. *Hydrogeol J* 26(5):1301–1324. <https://doi.org/10.1007/s10040-018-1795-1>
- Yang HF, Meng RF, Bao XL, Cao WG, Li ZY, Xu BY (2022) Assessment of water level threshold for groundwater restoration and over-exploitation remediation the Beijing-Tianjin-Hebei plain. *J Groundw Sci Eng* 10(2):113–127. <https://doi.org/10.19637/j.cnki.2305-7068.2022.02.002>
- Yi L, Deng CL, Tian LZ, Xu XY, Jiang XY, Qiang XK, Qin HF, Ge JY, Chen GQ, Su Q, Chen YP, Shi XF, Xie Q, Yu HJ, Zhu RX (2016) Plio-Pleistocene evolution of Bohai Basin (East Asia): demise of Bohai Paleolake and transition to marine environment. *Sci Rep* 6:29403. <https://doi.org/10.1038/srep29403>

- Yu LL, Ding YY, Chen F, Hou J, Liu GJ, Tang SN, Ling MH, Liu YZ, Yan Y, An N (2018) Groundwater resources protection and management in China. *Water Policy* 20(3):447–460. <https://doi.org/10.2166/wp.2017.035>
- Zhan YH, Guo HM, Wang Y, Li RM, Hou CT, Shao JL, Cui YL (2014) Evolution of groundwater major components in the Hebei plain: evidences from 30-year monitoring data. *J Earth Sci* 25(3):563–574. <https://doi.org/10.1007/s12583-014-0445-3>
- Zhang M, Wang MY, Liu B, Wan CY, Li W, Wang HM, Sun L, Wang HF, Qiao XJ (2015) A new model for forecasting total dissolved solids evolution using hydrodynamics parameters in regional deep confined aquifers of North China plain. *Environ Earth Sci* 73(12):7811–7823. <https://doi.org/10.1007/s12665-015-4145-9>
- Zheng CM, Liu J, Cao GL, Kendy E, Wang H, Jia YW (2010) Can China cope with its water crisis? perspectives from the North China plain. *Groundwater* 48(3):350–354. https://doi.org/10.1111/j.1745-6584.2010.00695_3.x
- Zhu CJ, Li WY, Hao ZC, Zhou JH, Yang WH (2006) Simulation of one-dimension contaminant transport in non-darcy flow field through low permeability porous media. *Earth Environ* 34(1):19–22. <https://doi.org/10.14050/j.cnki.1672-9250.2006.01.004>
- Zhu CJ, Wang HB, Zhou JH, Zhao XJ, Yang WH, Li SW (2007) Experiment and numerical simulation of contaminant transport in non-Darcy fluid field through low permeability porous media. *J Liaoning Tech Univ (Nat Sci)* 26(S2):266–268
- Zhu Q, Wen Z, Jakada H (2020) A new solution to transient single-well push-pull test with low-permeability non-Darcian leakage effects. *J Contam Hydrol* 234:103689. <https://doi.org/10.1016/j.jconhyd.2020.103689>
- Zuo WZ, Wan L (2006) Characteristics of down-movement of the fresh–saline groundwater interface in the plain region of Tianjin. *Hydrogeol Eng Geol* 2:13–18. <https://doi.org/10.16030/j.cnkiissn.10003665200602005>

Publisher's Note Springer Nature remains neutral with regard to jurisdictional claims in published maps and institutional affiliations.

Springer Nature or its licensor (e.g. a society or other partner) holds exclusive rights to this article under a publishing agreement with the author(s) or other rightsholder(s); author self-archiving of the accepted manuscript version of this article is solely governed by the terms of such publishing agreement and applicable law.